Research Papers

GREENSUSMATER

Greensusmater
Vol. 1, No. 2, December 2024
https://doi.org/10.62755/greensusmater.2024.1.2.44-50

Check for updates

Congo red dye adsorption using ZnAl layered double hydroxide fabricated using hydrothermal methods

Anisa Fitri[1] Febriwan Rizki Lumbanraja[1] Istiara Rizqillah Hanifah[1] Bayu Prasetya[1] Rizky Aflaha[2] Septia Eka Marsha Putra[3]

[1] *Department of Materials Engineering, Faculty of Industrial Technology, Institut Teknologi Sumatera, Terusan Ryacudu, Way Hui, Jati Agung, Lampung Selatan 35365, Indonesia*
[2] *Department of Physics, Faculty of Mathematics and Natural Sciences, Universitas Gadjah Mada, Sekip Utara, BLS 21, Yogyakarta 55281, Indonesia*
[3] *Department of Engineering Physics, Faculty of Industrial Technology, Institut Teknologi Sumatera, Terusan Ryacudu, Way Hui, Jati Agung, Lampung Selatan 35365, Indonesia*

Corresponding author: septia.marsha@tf.itera.ac.id

ARTICLE HISTORY: Received: August 31, 2024 | Revised: September 28, 2024 | Accepted: October 6, 2024

ABSTRACT

Industrial dye pollutants, particularly azo dyes like Congo red, pose sIndustrial dye pollutants, particularly azo dyes like Congo red, pose significant environmental and health risks due to their toxic and non-biodegradable nature. This study assesses ZnAl Layered Double Hydroxide (ZnAl LDH) as an effective adsorbent, incorporating comprehensive materials characterization and adsorption isotherm analyses. Materials characterization using SEM and XRD confirmed the structural integrity and morphological suitability of ZnAl LDH for dye adsorption. Results demonstrated that ZnAl LDH, particularly the HMTA-based variant (h-ZnAl LDH), achieved superior adsorption capacities of up to 17.8 mg/g, significantly outperforming the urea-based (u-ZnAl LDH) with capacity of 12.3 mg/g. Kinetic analysis showed that the pseudo-second-order (PSO) model provided a better fit (R^2 = 0.995) than the pseudo-first-order (PFO) model, indicating that chemisorption plays a dominant role in the adsorption mechanism. The adsorption process was also best described by the Langmuir isotherm model (R^2 = 0.989), indicating monolayer adsorption on a homogeneous surface, while the Freundlich model (R^2 = 0.944) also provided a reasonable fit, suggesting some degree of multilayer adsorption on heterogeneous surfaces. The superior performance of HMTA-based ZnAl LDH presents a significant advancement in wastewater treatment technologiesignificant environmental and health risks due to their toxic and non-biodegradable nature.

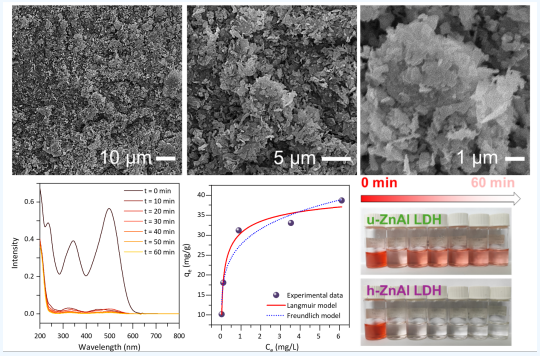

Keywords: *ZnAl LDH, hexamethylenetetramine, adsorption kinetics, isotherm, hydrothermal*

1. INTRODUCTION

Textile dyes, commonly composed of azo compounds and benzene groups, are a major class of non-biodegradable pollutants [1, 2]. Azo dyes are extensively used in textile manufacturing to create vibrant colors. After use, these dyes are often discarded into rivers or irrigation channels. Most organic dyes in textile industry wastewater possess aromatic structures, making them resistant to natural decomposition and potentially hazardous [3]. One such dye, Congo red, is known for its carcinogenic and mutagenic properties, posing significant health risks [4]. Thus, developing an efficient method to eliminate these pollutants from aquatic ecosystems is crucial [5, 6].

Various techniques, including sedimentation, filtration, coagulation, oxidation, electrochemistry, advanced oxidation processes (AOPs), biological methods, adsorption, ion exchange, photocatalysis, and piezo-photocatalysis, have been explored to mitigate the adverse effects of dye waste [7, 8, 9, 10, 11]. ZnAl Layered Double Hydroxide (ZnAl LDH) has emerged as a promising material in various dye removal technologies due to its unique layered structure and high anion-exchange capacity [12, 13]. This structure consists of positively charged brucite-like layers that can trap anions such as those found in azo dyes between the layers, making ZnAl LDH highly effective for dye adsorption. The material has been widely applied in adsorption techniques due to its capacity to remove both cationic and anionic dyes, including methyl orange, methylene blue, and Congo red, through ion exchange and surface adsorption processes [14, 15, 16].

Despite the proven efficiency of ZnAl LDH in various dye removal processes, the potential of its different synthesis methods and their impact on adsorption performance has not been thoroughly explored. This study aims to investigate the adsorption capabilities of ZnAl LDH synthesized using two different mineralizers namely hexamethylenetetramine (HMTA) and urea in the removal of Congo red, a widely used and hazardous azo dye. By comparing the performance of HMTA-based and urea-based ZnAl LDH, this research seeks to determine which variant exhibits superior adsorption capacity and kinetic behavior. The study also models

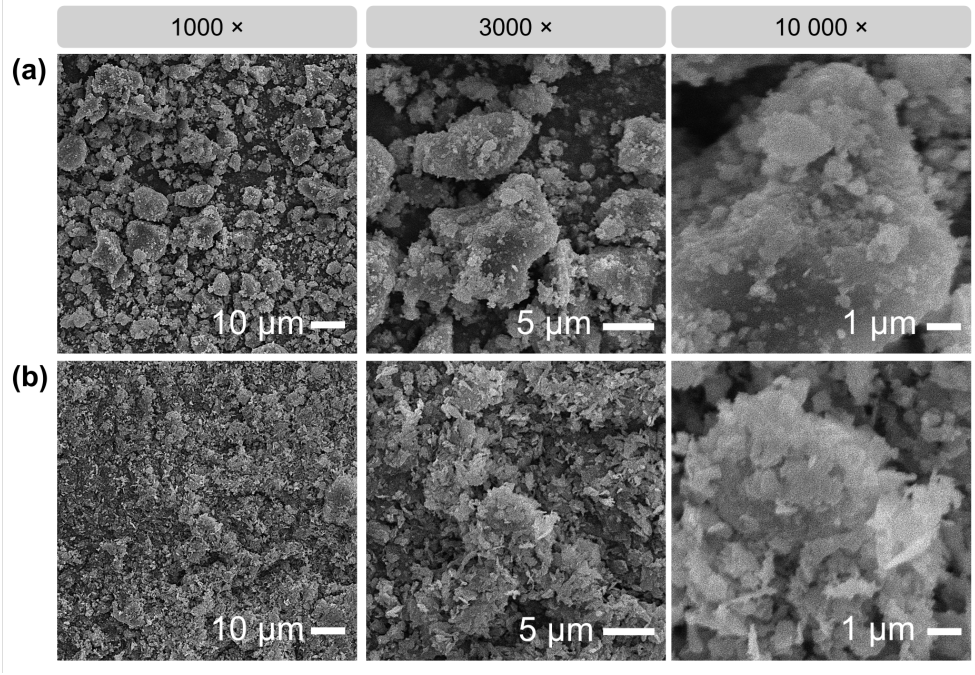

Element	Mass (wt%)	Atomic (wt%)
C	8.17	15.29
O	41.30	57.99
Al	19.15	15.94
Zn	31.37	10.78

Element	Mass (wt%)	Atomic (wt%)
C	9.28	29.45
O	33.95	53.39
Al	9.68	9.03
Zn	47.09	18.13

Figure 1. SEM images and corresponding EDS analysis of (a) u-ZnAl LDH and (b) h-ZnAl LDH samples

the adsorption kinetics using Pseudo-first-order (PFO) and Pseudo-second-order (PSO) models, as well as evaluates the adsorption isotherms to better understand the mechanism behind the dye removal. The findings are expected to contribute to the development of more efficient and scalable ZnAl LDH-based systems for industrial wastewater treatment.

2. MATERIAL AND METHODS

2.1 Materials

All precursor materials and chemicals including Zinc Nitrate Hexahydrate ($Zn(NO_3)_2 \cdot 6\,H_2O$), Aluminum Nitrate Nonahydrate ($Al(NO_3)_3 \cdot 9\,H_2O$), hexamethylenetetramine (HMTA), urea, and Congo red (CR, C.I. 22120) dye were purchased from Merck, Darmstadt, Germany.

2.2 Preparation of ZnAl Layered Double Hydroxide

The ZnAl layered double hydroxides were synthesized via a hydrothermal method similar to previous literature [17]. A precursor solution was prepared by dissolving 5.95 grams of $Zn(NO_3)_2 \cdot 6\,H_2O$ and 3.75 grams of $Al(NO_3)_3 \cdot 9\,H_2O$ in 70 mL of distilled water to achieve a molar ratio of 2:1. This solution was stirred at 500 rpm on a hot plate until the precursors fully dissolved, approximately 30 minutes. Two distinct mineralizer solutions were then prepared: one containing 3.65 grams of HMTA and another containing 1.65 grams of urea, each was added into the previous solutions and further stirred at 500 rpm for 30 minutes until homogeneous. These solutions were each transferred to separate 100-mL Stainless-steel Teflon-lined autoclaves, sealed, and heated at 140 °C for 24 hours. The resultant precipitates were vacuum filtered, washed with distilled water, and dried in an oven at 80 °C for 4 hours.

2.3 Materials characterizations

The synthesized materials were first characterized by Scanning Electron Microscopy equipped with Energy Dispersive X-ray Spectroscopy (SEM-EDS JEOL JSM-6510) to assess surface morphology and elemental composition. X-ray Diffractometry (XRD, Rigaku, SmartLab SE basic) was used to evaluate crystallinity, and Fourier Transform Infrared Spectroscopy (FTIR, Shimadzu IRSpirit-X Compact) was employed to identify chemical bonding and functional groups.

2.4 Adsorption investigations

The adsorption properties of the synthesized materials were investigated through a comprehensive study. Initially, the adsorption capacity of each catalyst, ZnAl-HMTA and ZnAl-Urea, was determined using a 10 ppm Congo red dye solution. For this, 0.05 grams of each catalyst was added to 100 ml of the dye solution, which was then stirred at 300 rpm on a hot plate stirrer. Samples of 5 ml were collected at intervals of 10 minutes for a duration of 60 minutes. These samples were analyzed using UV-Vis spectroscopy to assess the dye's adsorption. Subsequently, adsorption isotherm experiments were conducted using varying concentrations of Congo red dye, specifically at 5, 10, 15, 20, and 25 ppm. This series aimed to understand the adsorption behavior under different dye concentrations, following the same sampling and analytical procedures as the initial tests.

3. RESULTS AND DISCUSSION

3.1 ZnAl LDH characteristics

The SEM images presented in Figure 1(a) and (b) reveal distinct morphological differences between the u- and h-ZnAl LDH samples. Figure 1(a) shows the u-ZnAl LDH exhibited an irregular and agglomerated morphology, characterized by uneven and less defined structures, suggesting that the urea precursor leads to a less uniform nucleation and growth process under hydrothermal conditions [18]. In contrast, Figure 1(b) depicts the h-ZnAl LDH samples, in which exhibits a more uniform, "plate-like" morphology with better-defined particles [19, 20]. The consistent structure of the HMTA-based

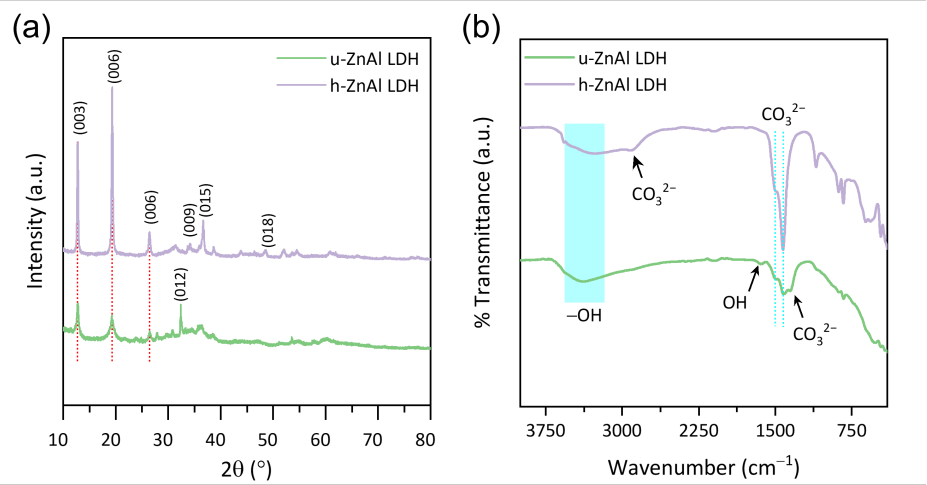

Figure 2. The (a) XRD and (b) FTIR analysis of the u-ZnAl LDH and h-ZnAl LDH samples

ZnAl LDH could be attributed to the more controlled decomposition of HMTA during synthesis, which promotes uniform nucleation and growth of the LDH crystals.

The accompanying EDS (Energy-Dispersive X-ray Spectroscopy) analysis provides insights into the elemental composition of the samples. The u-ZnAl LDH (Figure 1(a), right side) shows a Zn/Al atomic ratio of approximately 0.68:1, with zinc and aluminum atomic percentages of 10.78% and 15.94%, respectively. This ratio indicates a significant deviation from the targeted 2:1 ratio, with a lower zinc content and higher aluminum content than expected. This could suggest incomplete incorporation of zinc or over-incorporation of aluminum during the synthesis process. In contrast, the h-ZnAl LDH (Figure 1(b), right side) exhibits a Zn/Al atomic ratio of approximately 2.01:1, with zinc and aluminum atomic percentages of 18.13% and 9.03%, respectively. This ratio closely matches the desired 2:1 stoichiometry, indicating a more successful incorporation of zinc relative to aluminum in the LDH structure when using HMTA as a precursor [21].

The XRD patterns of the u-ZnAl LDH and h-ZnAl LDH samples are shown in Figure 2(a). The diffraction peaks observed in the h-ZnAl LDH sample correspond to the characteristic reflections of a well-formed layered double hydroxide structure, with sharp and intense peaks at 2θ values around 11.6 °, 23.3 °, 34.8 °, 39.3 °, and 60.8 °. These peaks can be indexed to the (003), (006), (012), (015), and (110) planes, respectively, indicating a high degree of crystallinity and a well-ordered layered structure with the Zn_2^+/Al_3^+ catopnic ratio of 2:1 [22, 23]. In contrast, the XRD pattern of the u-ZnAl LDH shows broader and less intense peaks. This suggests that the u-ZnAl LDH has a lower crystallinity compared to the h-ZnAl LDH. The peaks corresponding to the (003) and (006) planes are present but are less defined, indicating that the layered structure is less ordered, likely due to the irregular and agglomerated morphology observed in the SEM images. The lower crystallinity might also be a result of the Zn/Al ratio deviation from the ideal 2:1 stoichiometry, as previously discussed.

The FTIR spectra of the u-ZnAl LDH and h-ZnAl LDH are presented in Figure 2(b). Both spectra display characteristic absorption bands that correspond to the functional groups present in the ZnAl LDH structure [22]. For the h-ZnAl LDH, the broad absorption band around 3400 cm^{-1} is attributed to the OH stretching vibrations of the hydroxyl groups in the LDH layers and interlayer water molecules [24]. The band around 1638 cm^{-1} is due to the bending vibrations of water molecules in the interlayer [24]. The u-ZnAl LDH also exhibits similar band around 3400 cm^{-1} and 1638 cm^{-1}, but they are broader and less intense, reflecting the lower crystallinity and potentially less structured interlayer water in this sample. This aligns with the XRD results indicating poorer crystallinity in u-ZnAl LDH. The bands observed around 1500 cm^{-1} and 1380 cm^{-1} in both spectra correspond to the stretching vibrations of the interlayer carbonate anions, which are commonly present in LDHs due to their affinity for CO_2 from the atmosphere [25, 26]. However, the intensity of these bands is lower in the u-ZnAl LDH, which may be due to a lower degree of carbonate intercalation or less ordered layer stacking. The FTIR spectra also show bands in the 600–800 cm^{-1} range, corresponding to the M-O (metal-oxygen) and M-O-M (metal-oxygen-metal) stretching vibrations within the LDH layers [23, 27]. The h-ZnAl LDH shows more defined bands in this region, consistent with its higher crystallinity and better-ordered layered structure.

3.2 ZnAl LDH adsorption kinetics

In the analysis of Congo red dye adsorption, UV-Vis absorption spectra reveal key insights into the effectiveness of the catalysts over a 60-minute period. Figure 3(a) and (b) displays the absorption spectra for u-ZnAl LDH and h-ZnAl LDH, respectively. Initially, both catalysts show strong absorption peaks around 498 nm, indicative of the presence of Congo red dye. As time progresses, these peaks diminish, with h-ZnAl LDH demonstrating a more pronounced decrease in intensity, suggesting more effective dye adsorption compared to u-ZnAl LDH. This observation is visually supported by Figure 3(c), where the upper row showing u-ZnAl LDH and the lower row h-ZnAl LDH both depict a reduction in dye colour intensity. However, the colour fading is notably more significant in the h-ZnAl LDH samples, aligning with the quantitative data from the UV-Vis absorption spectra.

Figure 3(d) quantifies the adsorption capacity, calculate using Equation that available in literatures [28, 29]. The result illustrating a rapid increase in dye removal within the first 20 minutes for both catalysts, which then plateaus towards the 40-minute mark. Here, h-ZnAl LDH reaches a higher

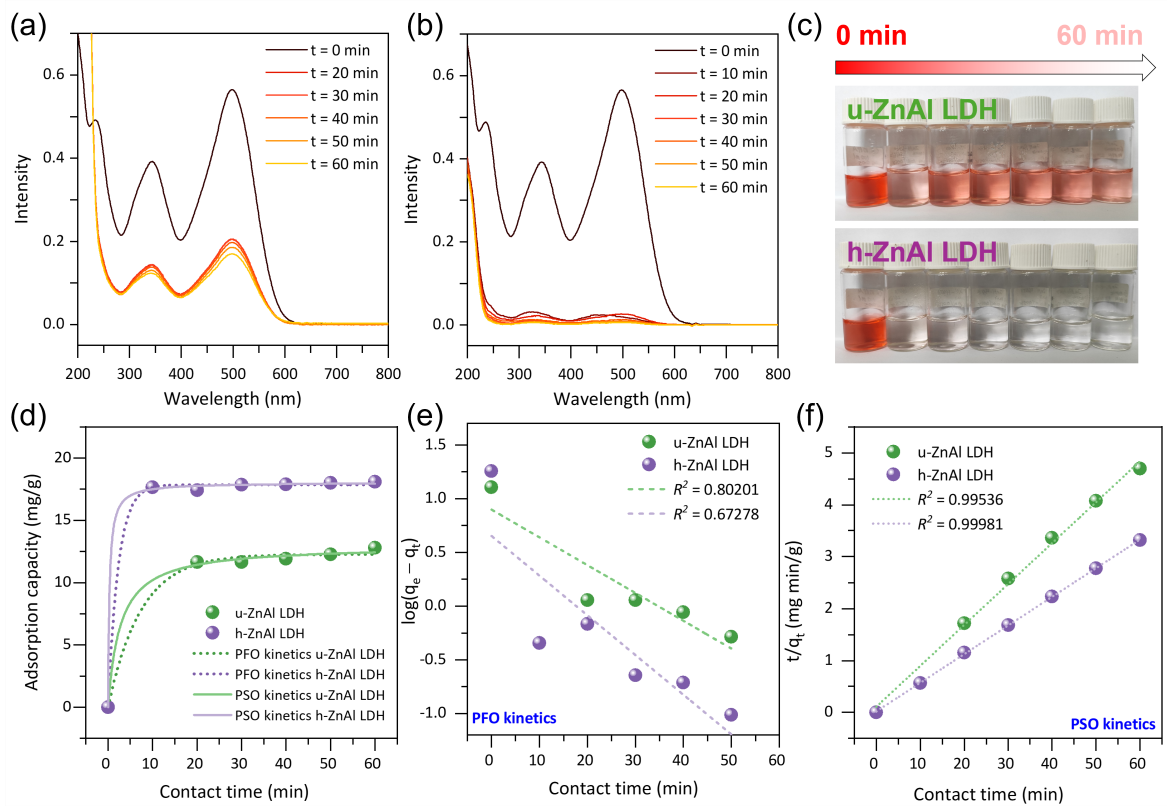

Figure 3. (a) UV-Vis absorption spectra for (a) u-ZnAl LDH and (b) u-ZnAl LDH sample over time (60 min). (c) Visual demonstration of dye adsorption; the upper row corresponds to u-ZnAl LDH and the lower row to h-ZnAl LDH, showing color intensity reduction over time. (d) Adsorption capacity of u-ZnAl LDH and h-ZnAl LDH as a function of contact time with fittings to PFO and PSO kinetic models. Linear fit plots for (e) PFO and (f) PSO kinetics.

equilibrium capacity (Qe) of 17.8 mg/g, compared to 12.3 mg/g for u-ZnAl LDH. The adsorption kinetics, analysed through pseudo-first-order (PFO) and pseudo-second-order (PSO) models, further elucidate the adsorption dynamics [30, 31, 32]. The PFO model shows a poorer fit to the data, especially for u-ZnAl LDH as seen in Figure 3(e). Sample shows a low R^2 value of 0.802 and 0.673 for u-ZnAL LDH and h-ZnAl LDH sample, respectively. Conversely, the PSO model, indicative of chemisorption involving shared or exchanged electrons between dye and catalyst, fits the experimental data exceptionally well for both catalysts with R^2 value higher than 0.995, as depicted in Figure 3(f). Overall, the analyses clearly demonstrate that h-ZnAl LDH is more effective than u-ZnAl LDH in adsorbing Congo red dye from aqueous solutions. The superior performance of h-ZnAl LDH is evident in both the visual and quantitative results and is further supported by kinetic modeling that confirms chemisorption as the predominant mechanism of dye removal. These findings highlight the potential of h-ZnAl LDH as a highly effective catalyst for environmental remediation applications, particularly in the treatment of wastewater containing dye pollutants.

3.3 ZnAl LDH adsorption isotherm

The adsorption behavior of Congo red dye onto ZnAl LDH was investigated using UV-Vis absorption spectra and modeled through adsorption isotherms. The UV-Vis spectra displayed in Figure 4(a) for different concentrations (5, 10, 15, 20, and 25 ppm) show a marked decrease in intensity over 60 minutes, signaling effective dye adsorption. The corresponding photographs within the panel visually confirm this trend, where a noticeable fading of the dye's color intensity is evident, especially prominent at higher concentrations. This indicates robust adsorption capabilities of ZnAl LDH, consistent across the tested dye concentration range.

Further quantification of the adsorption process is explored in Figure 4(b), (c), and (d) through Langmuir and Freundlich isotherm models [33, 34]. The experimental data plotted alongside the isotherm curves in Figure 4(b) fits both models well, suggesting simultaneous monolayer and potentially multilayer adsorption on heterogeneous sites. The Langmuir isotherm, depicted in Figure 4(c), shows a high correlation (R^2 = 0.98909) supporting a monolayer adsorption mechanism where each adsorbent site on the ZnAl LDH binds a single molecule of dye. This linear relationship emphasizes that ZnAl LDH provides specific, energetically uniform adsorption sites that become saturated without overlap once occupied.

Conversely, the Freundlich isotherm model presented in Figure 4(d) plots, yielding an R^2 value of 0.94382, indicative of multilayer adsorption on a heterogeneous surface. This model's fit suggests that ZnAl LDH also possesses a variety of adsorption sites with different binding energies, likely accommodating multiple layers of dye molecules. The effectiveness of both isotherm models implies complex adsorptive interactions on ZnAl LDH's surface, characterized by a combination of physical and chemical adsorption processes. Overall, the data illustrates that ZnAl LDH is a potent adsorbent for re-

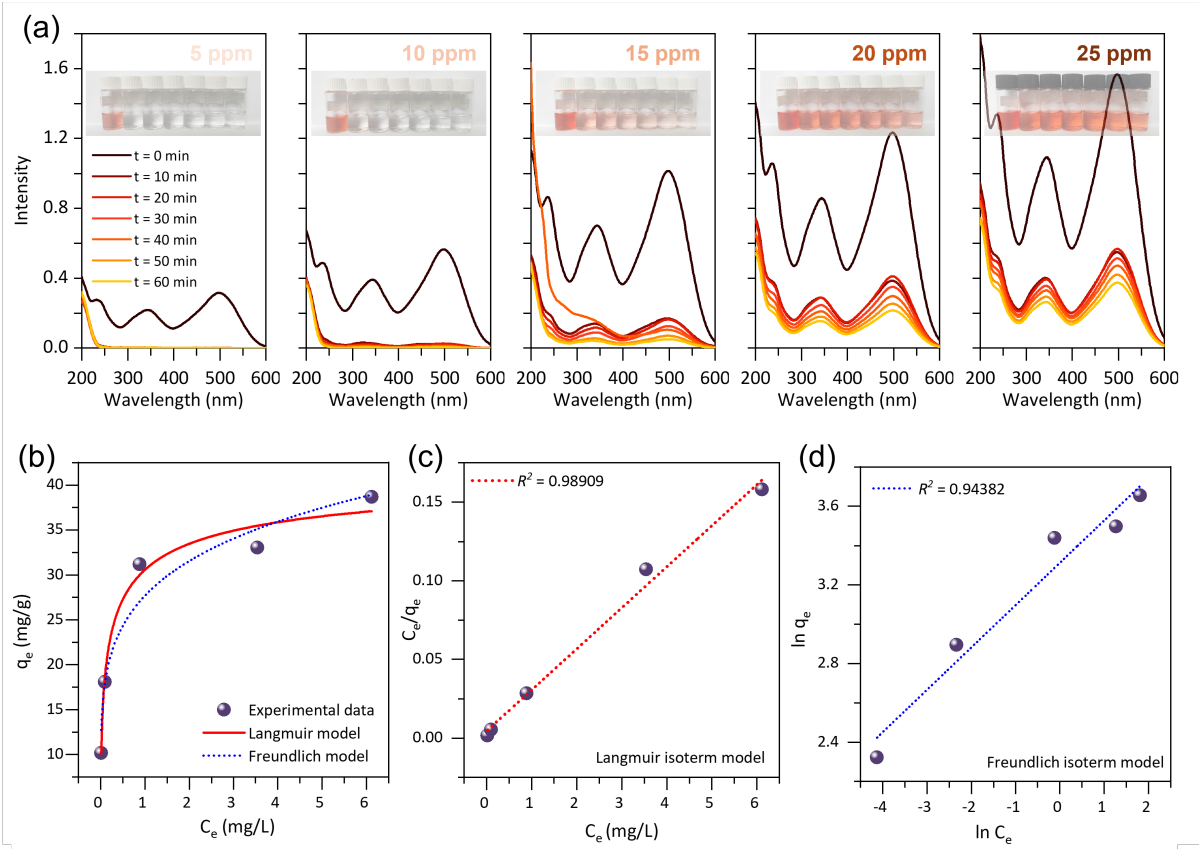

Figure 4. (a) UV-Vis absorption spectra at varying Congo red concentrations (5, 10, 15, 20, 25 ppm) over time (0 to 60 minutes), with inset photographs showing color change in dye solutions. (b) Experimental adsorption capacity (qe) plotted against equilibrium concentration (Ce), fitted with Langmuir and Freundlich isotherm models. The (c) Langmuir and (f) Freundlich isotherm plot of the CR adsorption on the h-ZnAl LDH surfaces

moving Congo red dye from aqueous solutions, validated by both visual and quantitative analyses. The congruence of the experimental results with Langmuir and Freundlich isotherms provides valuable insights into the nature of the adsorption mechanism, proposing that ZnAl LDH could be particularly effective in water treatment applications where comprehensive dye removal is essential.

4. CONCLUSION

This study aimed to evaluate the effectiveness of ZnAl Layered Double Hydroxide (ZnAl LDH) in adsorbing Congo red dye from aqueous solutions and to accurately model this process using Langmuir and Freundlich isotherms. Key findings demonstrated that ZnAl LDH effectively reduces dye concentrations, achieving up to 17.8 mg/g adsorption capacity at higher concentrations. The Langmuir isotherm provided a strong fit (R^2 = 0.98909), supporting monolayer adsorption, while the Freundlich isotherm, with an R^2 of 0.94382, indicated efficient multilayer adsorption on heterogeneous surfaces. These results highlight ZnAl LDH's potential for practical water purification applications. Future research should explore the optimization of ZnAl LDH synthesis to increase its cost-effectiveness and operational efficiency. Investigating the material's performance with different classes of industrial pollutants could further establish its versatility in broader environmental remediation applications, offering a significant step forward in wastewater treatment technologies.

CONFLICT OF INTEREST

The authors declare that there are no conflicts of interest.

DATA AVAILABILITY

The datasets generated and analyzed during the current study are available from the corresponding author upon reasonable request.

ACKNOWLEDGEMENT

This study receive no funding

REFERENCES

[1] S. Kasavan, S. Yusoff, N. C. Guan, N. S. K. Zaman, M. F. R. Fakri, Global trends of textile waste research from 2005 to 2020 using bibliometric analysis, Environmental Science and Pollution Research 28 (33) (2021) 44780–44794. https://doi.org/10.1007/s11356-021-15303-5.

[2] A. Rianjanu, K. D. P. Marpaung, C. Siburian, S. A. Muhtar, N. I. Khamidy, J. Widakdo, N. Yulianto, R. Aflaha, K. Triyana, T. Taher, Enhancement of photocatalytic activity of CeO2 nanorods through lanthanum doping (La–CeO2) for the degradation of Congo red dyes, Results in Engineering 23 (2024) 102748. https://doi.org/10.1016/j.rineng.2024.102748.

[3] P. K. Mishra, A. M. D. Izrayeel, B. K. Mahur, A. Ahuja, V. K. Rastogi, A comprehensive review on textile waste valorization techniques and their applications, Environmental Science and Pollution Research 29 (44) (2022) 65962–65977. https://doi.org/10.1007/s11356-022-22222-6.

[4] P. O. Oladoye, M. O. Bamigboye, O. D. Ogunbiyi, M. T. Akano, Toxicity and decontamination strategies of Congo red dye, Groundwater for Sustainable Development 19 (2022) 100844. https://doi.org/10.1016/j.gsd.2022.100844.

[5] M. Harja, G. Buema, D. Bucur, Recent advances in removal of Congo Red dye by adsorption using an industrial waste, Scientific Reports 12 (1) (2022) 6087. https://doi.org/10.1038/s41598-022-10093-3.

[6] A. Rianjanu, A. S. P. Mustamin, E. K. A. Melati, R. Aflaha, N. I. Khamidy, M. Utami, K. Khairurrijal, K. Triyana, F. F. Abdi, H. S. Wasisto, T. Taher, Photocatalytic degradation of aqueous Congo red dye pollutants by rare-earth metal oxide (CeO2) nanorods, Colloids and Surfaces A: Physicochemical and Engineering Aspects 682 (2024) 132919. https://doi.org/10.1016/j.colsurfa.2023.132919.

[7] R. R. M. Khan, H. Qamar, A. Hameed, A. U. Rehman, M. Pervaiz, Z. Saeed, A. Adnan, A. R. Ch, Biological and Photocatalytic Degradation of Congo Red, a Diazo Sulfonated Substituted Dye: a Review, Water, Air, & Soil Pollution 233 (11) (2022) 468. https://doi.org/10.1007/s11270-022-05935-9.

[8] Y. Patil, S. Attarde, R. Dhake, U. Fegade, A. M. A. Alaghaz, Adsorption of Congo red dye using metal oxide nanoadsorbents: Past, present, and future perspective, International Journal of Chemical Kinetics 55 (10) (2023) 579–605. https://doi.org/10.1002/kin.21675.

[9] K. Manzoor, M. Batool, F. Naz, M. F. Nazar, B. H. Hameed, M. N. Zafar, A comprehensive review on application of plant-based bioadsorbents for Congo red removal, Biomass Conversion and Biorefinery 14 (4) (2024) 4511–4537. https://doi.org/10.1007/s13399-022-02741-5.

[10] M. F. Arif, S. A. Muhtar, C. Siburian, K. D. P. Marpaung, N. Yulianto, F. F. Abdi, T. Taher, H. S. Wasisto, A. Rianjanu, Zeolite-PAN/PVDF composite nanofiber membranes for highly efficient and selective removal of cationic dyes from wastewater, Case Studies in Chemical and Environmental Engineering 10 (2024) 100806. https://doi.org/10.1016/j.cscee.2024.100806.

[11] A. Rianjanu, K. D. P. Marpaung, E. K. A. Melati, R. Aflaha, Y. G. Wibowo, I. P. Mahendra, N. Yulianto, J. Widakdo, K. Triyana, H. S. Wasisto, T. Taher, Integrated adsorption and photocatalytic removal of methylene blue dye from aqueous solution by hierarchical Nb2O5@PAN/PVDF/ANO composite nanofibers, Nano Materials Science 6 (1) (2024) 96–105. https://doi.org/10.1016/j.nanoms.2023.10.006.

[12] B. S. Marques, K. Dalmagro, K. S. Moreira, M. L. Oliveira, S. L. Jahn, T. A. De Lima Burgo, G. L. Dotto, Ca–Al, Ni–Al and Zn–Al LDH powders as efficient materials to treat synthetic effluents containing o-nitrophenol, Journal of Alloys and Compounds 838 (2020) 155628. https://doi.org/10.1016/j.jallcom.2020.155628.

[13] S. Yadav, A. Ahmad, C. Gulati, M. M. Ghangrekar, B. K. Dubey, Zn-Al@LDH infused hydrochar as cathode catalyst for upgrading tetracycline degradation and hospital wastewater treatment: A synergy of Fenton-like and bio-electrochemical systems, Journal of Environmental Chemical Engineering 12 (5) (2024) 113874. https://doi.org/10.1016/j.jece.2024.113874.

[14] J. Zheng, C. Fan, X. Li, Q. Yang, D. Wang, A. Duan, S. Pan, Tourmaline/ZnAL-LDH nanocomposite based photocatalytic system for efficient degradation of mixed pollutant wastewater, Separation and Purification Technology 345 (2024) 127306. https://doi.org/10.1016/j.seppur.2024.127306.

[15] H. Boumeriame, E. S. Da Silva, A. S. Cherevan, T. Chafik, J. L. Faria, D. Eder, Layered double hydroxide (LDH)-based materials: A mini-review on strategies to improve the performance for photocatalytic water splitting, Journal of Energy Chemistry 64 (2022) 406–431. https://doi.org/10.1016/j.jechem.2021.04.050.

[16] T. Taher, Z. Yu, E. K. A. Melati, A. Munandar, R. Aflaha, K. Triyana, Y. G. Wibowo, K. Khairurrijal, A. Lesbani, A. Rianjanu, Enabling dual-functionality material for effective anionic and cationic dye removal by using Nb2O5/MgAl-LDH nanocomposites, Journal of Hazardous Materials Letters 5 (2024) 100103. https://doi.org/10.1016/j.hazl.2024.100103.

[17] J. Hu, C. Yu, C. Li, S. Lan, L. Zeng, M. Zhu, Thickness-dependent piezo-photo-responsive behavior of ZnAl-layered double hydroxide for wastewater remediation, Nano Energy 101 (2022) 107583. https://doi.org/10.1016/j.nanoen.2022.107583.

[18] N. Ahmad, F. Suryani Arsyad, I. Royani, P. Mega Syah Bahar Nur Siregar, T. Taher, A. Lesbani, High regeneration of ZnAl/NiAl-Magnetite humic acid for adsorption of Congo red from aqueous solution, Inorganic Chemistry Communications 150 (2023) 110517. https://doi.org/10.1016/j.inoche.2023.110517.

[19] T. Taher, A. Munandar, N. Mawaddah, M. Syamsuddin Wisnubroto, P. M. S. B. N. Siregar, N. R. Palapa, A. Lesbani, Y. G. Wibowo, Synthesis and characterization of montmorillonite – Mixed metal oxide composite and its adsorption performance for anionic and cationic dyes removal, Inorganic Chemistry Communications 147 (2023) 110231. https://doi.org/10.1016/j.inoche.2022.110231.

[20] M. Pedraza-Chan, U. Salazar-Kuri, R. Sánchez-Zeferino, I. Ruiz-López, A. Escobedo-Morales, Emulation of evolutionary selection as the growth mechanism of supported layered double hydroxide frameworks, Applied Clay Science 210 (2021) 106159. https://doi.org/10.1016/j.clay.2021.106159.

[21] K. Manjula Rani, P. N. Palanisamy, Synthesis and Characterization of Mesoporous, Nanostructured Zinc Aluminium Carbonate Layered Double Hydroxides (ZAC-LDHs) and Its Calcined Product (CZA-LDH), Journal of Inorganic and Organometallic Polymers and Materials 28 (3) (2018) 1127–1135. https://doi.org/10.1007/s10904-018-0796-9.

[22] A. A. A. Ahmed, Z. A. Talib, M. Z. Bin Hussein, A. Zakaria, Zn–Al layered double hydroxide prepared at different molar ratios: Preparation, characterization, optical and dielectric properties, Journal of Solid State Chemistry 191 (2012) 271–278. https://doi.org/10.1016/j.jssc.2012.03.013.

[23] A. Li, H. Deng, C. Ye, Y. Jiang, Fabrication and Characterization of Novel ZnAl-Layered Double Hydroxide for the Superadsorption of Organic Contaminants from Wastewater, ACS Omega 5 (25) (2020) 15152–15161. https://doi.org/10.1021/acsomega.0c01092.

[24] G. Starukh, O. Rozovik, O. Oranska, Organo/Zn-Al LDH Nanocomposites for Cationic Dye Removal from Aqueous Media, Nanoscale Research Letters 11 (1) (2016) 228. https://doi.org/10.1186/s11671-016-1402-0.

[25] L. Liu, M. Cheng, Z. Yang, Improved performance of flower-like ZnAl LDH growing on carbon nanotubes used in zinc–nickel secondary battery, Electrochimica Acta 277 (2018) 67–76. https://doi.org/10.1016/j.electacta.2018.04.201.

[26] J. Hu, M. Gan, L. Ma, J. Zhang, S. Xie, F. Xu, J. Z. X. Shen, H. Yin, Preparation and enhanced properties of polyaniline/grafted intercalated ZnAl-LDH nanocomposites, Applied Surface Science 328 (2015) 325–334. https://doi.org/10.1016/j.apsusc.2014.12.042.

[27] D. Téllez-Flores, M. Sánchez-Cantú, F. Tzompantzi, A. G. Romero-Villegas, C. Tzompantzi-Flores, J. E. Carrera-Crespo, R. Pérez-Hernández, E. Rubio-Rosas, Influence of the Zn/Al molar ratio over the photocatalytic hydrogen production by ZnS/ZnAl-LDH composites, International Journal of Hydrogen Energy (2024) S0360319924000788https://doi.org/10.1016/j.ijhydene.2024.01.069.

[28] C. Cai, R. Wang, S. Liu, X. Yan, L. Zhang, M. Wang, Q. Tong, T. Jiao, Synthesis of self-assembled phytic acid-MXene nanocomposites via a facile hydrothermal approach with elevated dye adsorption capacities, Colloids and Surfaces A: Physicochemical and Engineering Aspects 589 (2020) 124468. https://doi.org/10.1016/j.colsurfa.2020.124468.

[29] Q. Wang, C. Luo, Z. Lai, S. Chen, D. He, J. Mu, Honeycomb-like cork activated carbon with ultra-high adsorption capacity for anionic, cationic and mixed dye: Preparation, performance and mechanism, Bioresource Technology 357 (2022) 127363. https://doi.org/10.1016/j.biortech.2022.127363.

[30] Q. Hu, S. Pang, D. Wang, In-depth Insights into Mathematical Characteristics, Selection Criteria and Common Mistakes of Adsorption Kinetic Models: A Critical Review, Separation & Purification Reviews 51 (3) (2022) 281–299. https://doi.org/10.1080/15422119.2021.1922444.

[31] M. Verma, I. Tyagi, V. Kumar, S. Goel, D. Vaya, H. Kim, Fabrication of GO–MnO2 nanocomposite using hydrothermal process for cationic and anionic dyes adsorption: Kinetics, isotherm, and reusability, Journal of Environmental Chemical Engineering 9 (5) (2021) 106045. https://doi.org/10.1016/j.jece.2021.106045.

[32] R. Ezzati, S. Ezzati, M. Azizi, Exact solution of the Langmuir rate equation: New Insights into pseudo-first-order and pseudo-second-order kinetics models for adsorption, Vacuum 220 (2024) 112790. https://doi.org/10.1016/j.vacuum.2023.112790.

[33] M. Saxena, N. Sharma, R. Saxena, Highly efficient and rapid removal of a toxic dye: Adsorption kinetics, isotherm, and mechanism studies on functionalized multiwalled carbon nanotubes, Surfaces and Interfaces 21 (2020) 100639. https://doi.org/10.1016/j.surfin.2020.100639.

[34] S. Debnath, R. Das, Strong adsorption of CV dye by Ni ferrite nanoparticles for waste water purification: Fits well the pseudo second order kinetic and Freundlich isotherm model, Ceramics International 49 (10) (2023) 16199–16215. https://doi.org/10.1016/j.ceramint.2023.01.218.

